62. Mitry RR, Dhawan A, Hughes RD, Bansal S, Lehec S, Terry C, et al. One liver, three recipients: segment IV from split-liver procedures as a source of hepatocytes for cell transplantation. Transplantation 2004;77:1614–6.
63. Muraca M, Gerunda G, Neri D, Vilei MT, Granato A, Feltracco P, et al. Hepatocyte transplantation as a treatment for glycogen storage disease type 1a. Lancet 2002;359:317–8.
64. Sokal EM, Smets F, Bourgois A, Van Maldergem L, Buts JP, Reding R, et al. Hepatocyte transplantation in a 4-year-old girl with peroxisomal biogenesis disease: technique, safety, and metabolic follow-up. Transplantation 2003;76:735–8.
65. Horslen SP, Fox IJ. Hepatocyte transplantation. Transplantation 2004;77:1481–6.

J Hepatobiliary Pancreat Surg (2005) 12:386–390
DOI 10.1007/s00534-005-0984-1

Journal of HBP Surgery

Surgeon at work

Placement of a double-pigtail ERBD tube after primary closure of the common bile duct in three patients with choledocholithiasis

Masakazu Fujii[1], Motonori Okino[1], Kentaro Fujioka[1], Katsuyuki Yamashita[1], and Kimikazu Hamano[2]

[1]Department of Surgery, Onoda City Hospital, 1863-1 Higashitakatomari, Onoda, Yamaguchi 756-0094, Japan
[2]First Department of Surgery and Department of Digital Bio-information Medicine, Yamaguchi University, School of Medicine, Yamaguchi, Japan

Abstract
We devised a procedure for the placement of a double-pigtail endoscopic retrograde biliary drainage (ERBD) tube as an alternative to the placement of a T-tube. We used the procedure, after primary closure of the common bile duct, in three patients undergoing surgery for choledocholithiasis. All three patients were in their eighties, and all were diagnosed with cholecystolithiasis and choledocholithiasis. In all three, there were concerns about possible complications with the use of a T-tube. Two of the patients were senile and were thought to be likely to pull out the tube, and incomplete fistulation was considered possible in the third patient. Thus, there was an increased risk of bile peritonitis in all three patients. Placement of the ERBD tube was successful in all three patients, and there were no postoperative complications. The hospital stay was a few weeks shorter than the usual stay with the placement of a T-tube. We conclude that primary closure of the common bile duct with the placement of a double-pigtail ERBD tube is clinically safe and advantageous for choledocholithiasis patients with senile dementia and for patients with possible incomplete fistulation.

Key works Primary closure of CBD · Double-pigtail ERBD tube · Bile drainage · Cholerrhagia · Bile peritonitis

Introduction

Choledocholithotomy followed by T-tube drainage has long been a standard surgical treatment for choledocholithiasis. However, T-tube drainage can cause complications such as bile peritonitis. This is particularly true in patients with senile dementia (who may pull out the T-tube) and in patients in whom the fistula may fail to form completely, with both scenarios leading to bile peritonitis. Therefore, we devised a procedure for the placement of a double-pigtail endoscopic retrograde biliary drainage (ERBD) tube as an alternative to the placement of a T-tube. In the procedure, a Nélaton catheter (Izumohealth, Nagano, Japan) is inserted from the opening of the common bile duct through the ampulla of Vater into the duodenum. A guidewire is passed through the Nélaton catheter. The double-pigtail ERBD tube is inserted along the guidewire. The guidewire is removed, and the double-pigtail ERBD tube is placed in the common bile duct. The method was successful in all three patients in whom it was attempted, and there were no postoperative complications. Placement of the tube is done endoscopically, so we consider the surgical technique to be safe.

Offprint requests to: M. Fujii

This article is based on a study first reported in the Nihon Syokakigeka Gakkaizasshi (Jpn J Gastroenterol Surg) 2004;37:252–6.
Received: November 6, 2004 / Accepted: March 31, 2005

Case 1

An 88-year-old woman with fever and vomiting was diagnosed with cholecystolithiasis and choledocholithiasis. Removal of bile stones by endoscopic sphincteroctomy (EST) was not possible because of cannulation difficulty, so surgical treatment was considered. The patient's Japan Society of Clinical Oncology performance status was 4. It was thought that this patient, who had senile dementia, might pull out the T-tube, thus inducing bile peritonitis. Cholecystectomy and choledocholithotomy were performed, and the common bile duct was closed, with the placement of a double-pigtail ERBD tube (Fig. 1a). The common bile duct was dilated to a diameter of 18 mm. There were nine stones in the gallbladder: two that were approximately 25 mm in diameter and seven that were approximately 10 mm in diameter. There were also three stones in the common bile duct: one that was 15 mm in diameter and two that were approximately 5 mm in diameter. The ERBD tube was removed endoscopically (Fig. 1b)

The FASEB Journal • FJ Express

Reconstruction of 3D stacked-up structures by rat small hepatocytes on microporous membranes

Ryo Sudo,*[,1] Toshihiro Mitaka,[†] Mariko Ikeda,* and Kazuo Tanishita*

*Center for Life Science and Technology, School of Fundamental Science and Technology, Keio University, Yokohama, Japan; and [†]Department of Pathophysiology, Cancer Research Institute, Sapporo Medical University School of Medicine, Sapporo, Japan

To read the full text of this article, go to http://www.fasebj.org/cgi/doi/10.1096/fj.04-3269fje; doi: 10.1096/fj.04-3269fje

SPECIFIC AIMS

In this study we developed a simple 3-dimensional (3D) culture method that mimics the structure of hepatic cords by stacking up 2-dimensional (2D) tissues of rat small hepatocytes (SHs), which are hepatic progenitor cells. To evaluate the organization of the cells in 3D stacked-up structures, we ascertained whether the cells adhered to each other, formed bile canaliculi (BC) in the attached portions, and increased their liver-specific functions.

PRINCIPAL FINDINGS

1. 3D stacked-up culture of SHs

For the reconstruction of 3D hepatic organoids it is important to organize the cells into a tissue resembling liver architecture. Although it seems clear that 3D culture of hepatocytes must maintain hepatic differentiated functions, there is no feasible method to reconstruct 3D tissues. We therefore developed a simple 3D culture technique. The schematic diagram shown in **Fig. 1** summarizes 3D stacked-up structures produced by SHs and nonparenchymal cells (NPCs). In the present experiment SHs were isolated from adult rat livers. Pairs of microporous membranes were prepared and the cells were separately cultured on each membrane (Fig. 1*A*). SHs could proliferate and form colonies on the membranes, and the colonies gradually developed over time in culture. NPCs such as stellate cells also proliferated and surrounded the colonies. Then the stellate cells translocated beneath the colonies and some cells infiltrated under the membranes through the micropores. After SHs were cultured on the membranes for ~20 days and allowed to develop, one membrane was inverted on top of the other to form an SH bilayer. Thus, the 3D stacked-up structures could be reconstructed.

2. Cell adhesion and bile canalicular formation in the 3D stacked-up structures

To investigate the organization of the cells after stacking, bile canalicular formation in the 3D stacked-up structures was examined using fluorescein diacetate (FD). FD is metabolized in hepatocytes, and becomes fluorescein when secreted into BC. FD treatment revealed that BC formation started 3 days after stacking. Short BC then formed between the cells in the 3D stacked-up structures. The BC gradually elongated with the culture time and developed into anastomosing networks within 2 wk (Fig. 1*B*).

For the reconstruction of well-assembled 3D tissues, BC formation needs to occur in the attached portions between the cells of the upper and lower layers. We therefore labeled the cells of each layer with DiI and GFP to distinguish them in the 3D stacked-up structures. Fluorescent microscopy revealed that BC formed in the 3D stacked-up structures in which GFP-labeled cells were stacked onto the DiI-labeled cells, whereas no bile canalicular formation was identified in regions when both sides of the cells remained unattached. Although it is possible that the BC formation occurred in the region between the neighboring cells on each side, this was difficult to confirm using the labeling method described.

We then analyzed vertical sections of the 3D stacked-up structures using transmission electron microscopy. Perpendicular sections of the stacked cells showed that the hepatocytes of the upper and lower layers adhered to each other and formed a bilayer that was sandwiched between the membranes (**Fig. 2*A*, *C***). Between the cells of the upper and lower layers, a well-developed bile canaliculus was observed that formed a tubular structure (arrows, Fig. 2*A*). As shown in the enlarged image in Fig. 2*B*, the BC was ~1 μm in diameter and possessed many microvilli. Cell-cell junctions, such as tight junctions and desmosomes, were observed around the tubular structures (Fig. 2*B, D*).

3. Repolarization of the cells in the 3D stacked-up structures

Membrane polarity of SHs in the 3D stacked-up structures was also examined. Double fluorescent immunocyto-

[1] Correspondence: Center for Life Science and Technology, School of Fundamental Science and Technology, Keio University, 3-14-1 Hiyoshi, Kohoku-ku, Yokohama, 223-8522, Japan. E-mail: rsudo@2000.jukuin.keio.ac.jp

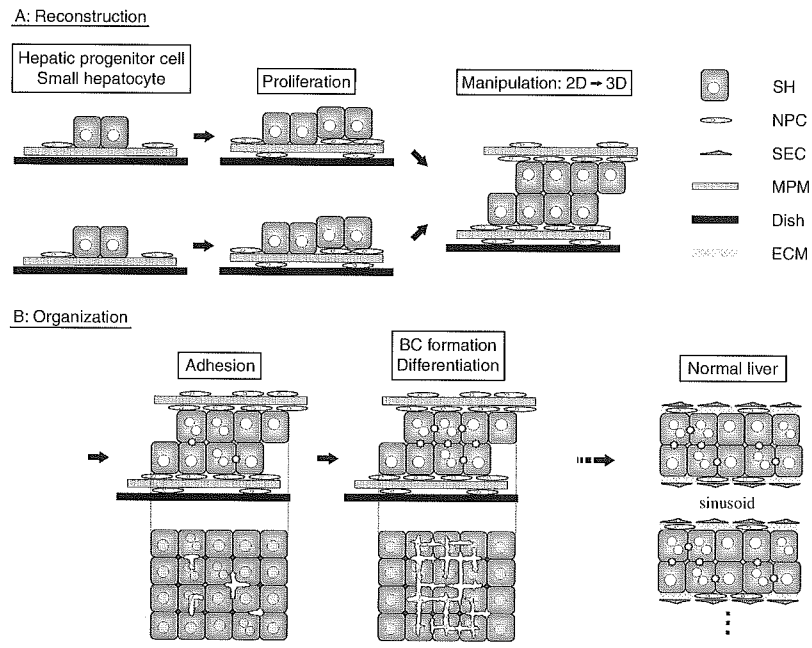

Figure 1. Schematic diagram of a 3D stacked-up culture. A combination of SHs and the stepwise progression from 2D to 3D successfully achieved the reconstruction of well-organized hepatic organoids. The process is divided into 2 stages: reconstruction (*A*) and organization (*B*). *A)* Initially, a single SH proliferates and forms a colony on each microporous membrane (MPM), which is then separately cultured in order to produce the structures. After the cells were cultured on the MPM and allowed to develop, they were stacked up. Thus, 3D stacked-up structures were reconstructed. *B)* After manipulation, the SHs of the upper and lower layers adhere to each other. Subsequently, BC start to form between the hepatocytes of the upper and lower layers, as well as between horizontally neighboring cells. Thereafter, the short BC gradually elongate and develop into anastomosing networks. Thus, the cells were organized into tissues in the 3D stacked-up structures. The resulting structures are histologically similar to those of a normal liver.

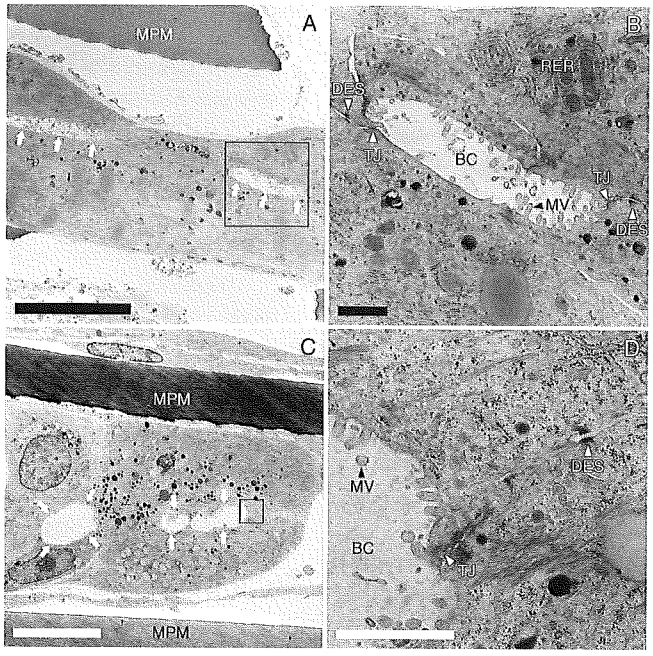

Figure 2. Electron micrographs of vertical sections of the 3D stacked-up structures. *A)* The cells were stacked at day 19 and fixed 24 days after stacking. The upper and lower layers adhere to each other to form a bilayer sandwiched by the microporous membranes (MPMs). Tubular BC are observed between the cells of the upper and lower layers (arrows). *B)* An enlarged image of the region indicated by the box in panel *A*. BC with luminal microvilli (MV) are formed between the cells, and are bounded both by tight junctions (TJ) and desmosomes (DES). Rough endoplasmic reticulum (RER) is visible within the cells. *C)* The cells were stacked at day 31 and fixed 48 days after stacking. Dilated BC were observed (arrows). NPCs with flat shapes were observed between the hepatocytes and the membranes, as well as on the membranes. *D)* An enlarged image of the region indicated by the box in panel *C*. The dilated BC possess MV and maintain the cell-cell junctions, such as TJ and DES. Scale bars: 10 μm (*A, C*) and 1 μm (*B, D*).

chemistry was carried out for actin and bile canalicular proteins, such as ectoATPase, multidrug resistance-associated protein 2 (MRP2), and 5′-nucleotidase (**Fig. 3**). The results show that these proteins localized on the lumina of BC within the 3D stacked-up structures. Actin filaments were abundant on the outer surface of the tubular structures. These results indicate that bile canalicular proteins localized on the extracellular side of the apical membrane and that actin filaments accumulated beneath the apical membrane. Therefore, hepatocytes in the 3D stacked-up structures might acquire membrane polarity. Our findings indicate that the reconstructed BC were morphologically and functionally similar to BC in vivo.

4. Albumin secretions and gene expression of the hepatic differentiation markers

Hepatic differentiated functions of the cells were examined as well as morphogenesis after stacking. The albumin secretions produced by the cells before and after stacking were measured using an ELISA. When the cells were stacked up, the amount of albumin secreted into the medium rapidly increased within 2 days and remained high for >2 wk. By contrast, the level of albumin secretion gradually diminished in the cells that were cultured on a membrane without stacking. We next examined whether the cells within the 3D stacked-up structures could express other differentiation markers. Reverse transcription-polymerase chain reaction analysis revealed that the mRNA expression of hepatocyte nuclear factor 4 (HNF-4) and tyrosine aminotransferase (TAT) were stronger in stacked cells than those in cells not stacked, though both cells expressed albumin and MRP2 mRNAs. mRNA expression of a highly differentiated marker, tryptophan-2, 3-dioxygenase (TO) in stacked cells was much stronger than those in cells that were not stacked.

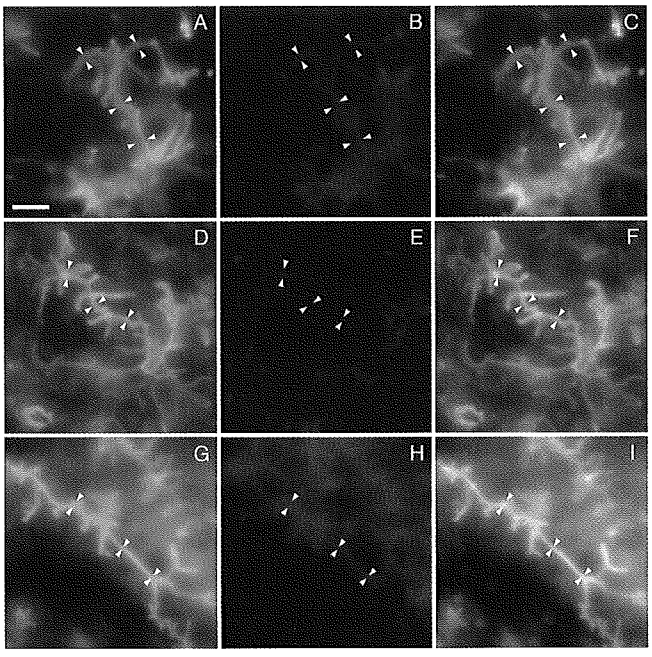

Figure 3. Localization of bile canalicular proteins and actin in the cells within the 3D stacked-up structure. The membranes were stacked at day 25 (*A–C*) or day 20 (*D–I*), and fixed 15 days after stacking. Triple immunostaining was carried out for bile canalicular proteins (green), actin (red), and DAPI (blue). The corresponding bile canalicular proteins (*A*, ectoATPase; *D*, MRP2; *G*, 5′NT), actin (*B, E, H*), and merged (*C, F, I*) images were taken using the 3D deconvolution microscopy. The branching tubular structures consist of an inner layer of ecto-ATPase and an outer layer of actin (arrowheads, *A–C*). MRP2 (arrowheads, *D–F*) and 5′NT (arrowheads, *G–I*) also localize along the tubular structures. The images were 3-dimensionally reconstructed by calculating 26 (*A–C*), 24 (*D–F*), and 22 (*G–I*) planes at 0.65 μm intervals. Scale bar: 20 μm.

CONCLUSIONS AND SIGNIFICANCE

In the field of tissue engineering of the liver, it is still unclear how we can reconstruct a complicated tissue maintaining various functions and how hepatocytes can proliferate and maintain their differentiated functions in vitro. Although primary hepatocytes rapidly lose their liver-specific functions in vitro, SHs can proliferate on the membrane and differentiate into mature hepatocytes (MHs). SHs are therefore considered suitable for the reconstruction of functional tissues. Tissue engineering is needed to reconstruct well-organized 3D tissues. Although 3D culture methods, such as hepatocyte spheroids and cultures in 3D scaffolds, have been reported, the formation of the tissues depends on the spontaneous behavior of the cells. Hepatocytes in vivo construct hepatic cords; organization of the cells is achieved by the interaction of MHs, NPCs, and extracellular matrix (ECM) whereas spheroids are simple aggregates composed of MHs alone. Considering the complex structure of the liver, it might be difficult to reconstruct well-assembled tissue depending on the spontaneous behavior. Therefore, precise manipulation of the cells is necessary to facilitate tissue organization. In the present experiment we created a simple 3D culture method that could reconstruct 3D stacked-up tissues from 2D structures. Within these structures, the SHs could organize themselves into orchestrated tissues with liver-specific functions. These results suggest that the combination of SHs and the stepwise progression from 2D to 3D is important for the reconstruction of well-organized hepatic organoids.

The structure of the normal liver is composed of continuous stacked cell layers (Fig. 1*B*). Hepatocytes form the hepatic cords, which are interconnected lines of cells. The strategy of the 3D stacked-up culture was to mimic these structures. In the present experiment we reconstructed 3D stacked-up structures in which the cells physiologically adhered and formed functional BC. These structures mimicked those of the hepatic cords. The cells could extend 3-dimensionally while maintaining both cell-cell and cell-ECM contacts. When SHs were sparsely inoculated onto collagen-coated dishes, they only attached onto the surface of the dish and did not maintain their cell-cell interactions. As a result, the cells extended 2-dimensionally and the cells became flat. By contrast, SHs in the 3D stacked-up structures could maintain both vertical and horizontal cell-cell interactions, as well as cell-ECM interactions. In vivo, hepatocytes seem to maintain their liver-specific function by forming 3D complex architectures interacting with NPCs and the ECM. Such microarchitectures might enhance the differentiation of SHs through maintenance of the cuboidal cell shape. In the present experiment, albumin secretion by the cells in the 3D stacked-up structures was enhanced compared with that in the cells on the membranes. In addition, the microarchitecture in the 3D stacked-up structures might also enhance the synthesis of liver-specific mRNAs, such as MRP2, HNF-4, TAT, and TO. Thus, the SHs achieved liver-specific functions by assembling into an appropriate configuration. The 3D stacked-up structures are not only similar to the structures of the hepatic lobules but also maintain their differentiated functions.

Liver transplantation is the only treatment for end-stage liver diseases, but donor organ shortages are a serious issue. Therefore, many researchers have attempted to restore liver function using bioartificial liver (BAL). Various cell types have been examined for use in the BAL reactor, but it is extremely difficult to maintain hepatocyte function in vitro. Therefore, tissue-engineered livers can be an alternative source for the BAL. In the present experiment, the cells were stacked onto those cultured on the membrane, which suggests the potential for multiple stacking; although only two membranes were stacked in the present experiment, three were successfully stacked in the preliminary study. Although further improvements will be necessary to achieve thicker complex tissues, the 3D stacked-up culture described here will be useful in the construction of tissue-engineered livers. FJ

The FASEB Journal • FJ Express

A critical role of a carboxylate in proton conduction by the ATP-binding cassette multidrug transporter LmrA

Richard Shilling,* Luca Federici,†,[1] Fabien Walas,† Henrietta Venter,* Saroj Velamakanni,* Barbara Woebking,* Lekshmy Balakrishnan,* Ben Luisi,† and Hendrik W. van Veen*,[2]

*Department of Pharmacology and †Department of Biochemistry, University of Cambridge, Cambridge, UK

To read the full text of this article, go to http://www.fasebj.org/cgi/doi/10.1096/fj.04-3558fje; doi: 10.1096/fj.04-3558fje

SPECIFIC AIMS

LmrA from *Lactococcus lactis* is a homologue of the human multidrug resistance P-glycoprotein MDR1 (ABCB1). Earlier work focused on the role of a carboxylate (E314) in proton-dependent ethidium transport by LmrA. The functional importance of this residue was suggested by its conservation in a wider family of related ABC transporters, but the structural basis of its role was not apparent. Here, we used homology modeling and functional analyses of LmrA mutants to define the structural environment of this key residue.

PRINCIPAL FINDINGS

1. Structural environment of E314

The crystal structure of MsbA from *Vibrio cholera* was used as a template to model LmrA-MD. The final model of LmrA-MD superimposes very well with the template, and all secondary structure elements are conserved, though they may vary in length. The root mean squared deviation between equivalent Cα atoms in the superimposed structures is 0.57 Å, which reflects the excellent quality of the model. LmrA-MD contains six extended transmembrane helices per monomer with different orientations with respect to the lipid bilayer normal. The extracellular loops (ECLs) are short, ranging from 3 residues in ECL2 to 9 residues in ECL1. The intracellular portions connecting transmembrane helices 2 and 3, and 4 and 5, and the linker region between transmembrane helix 6 and the NBD, together form the so-called intracellular domain (ICD) and are predominantly α-helical with the exception of a long extended region in ICD3.

Given the evidence supporting the LmrA-mediated transport of cationic amphiphilic substrates from the inner leaflet of the phospholipid bilayer, we searched for acidic residues in LmrA-MD with a favorable orientation to interact with cationic drugs from the inner membrane leaflet. The transmembrane helices of LmrA-MD form a principal groove that is proposed to be the site of substrate binding in MsbA. At the center of this groove in LmrA-MD, between the TM6 and its helical extension into ICD3, we have identified E314 as the first residue of an α-helix at the beginning of ICD3 (**Fig. 1*A*, *B***) in a hydrophobic micro-environment formed by L107 in ICD1, and F311 and L315 in ICD3 (Fig. 1*C*). E314 is conserved in MsbA from *V. cholera*, and the N- and C-terminal halves of human and murine P-glycoprotein. The residue is also present in the N-terminal, but not the C-terminal half of the human bile salt export pump (BSEP, also termed ABCB11), and in HorA from *Lactobacillus brevis* (Fig. 1*D*). As E314 is located close to the interface between the lipid bilayer and the cytoplasm, it is in a favorable position to intercept the cationic moiety of a drug intercalated in the inner leaflet of the membrane (Fig. 1*B*). E314 is also in a favorable position to play a role in the conformational coupling between the ATP binding/hydrolysis at the NBD and substrate movement by the MD in the same half-transporter, as TM6 is connected to the ATP-hydrolyzing NBD via the ICD3 region. In addition, both in the crystal structures of dimeric *V. cholera* MsbA and *Salmonella typhimurium* MsbA, and in a *V. cholera* MsbA-based model for human P-glycoprotein, the ICD3 region of one half-transporter is intimately packed to the NBD of the other half-transporter through its terminal extended coil. This suggests that any conformational change in the NBD region involving ATP binding and/or hydrolysis

[1] Current address: Ce.S.I. Centro Studi sull'Invecchiamento e Dipartimento di Scienze Biomediche, Universita' di Chieti "G. D'Annunzio," Via dei Vestini 31, 66013 Chieti, Italy.

[2] Correspondence: Department of Pharmacology, University of Cambridge, Tennis Court Road, Cambridge CB2 1PD, UK. E-mail: hwv20@cam.ac.uk

0892-6638/05/0019-1698 © FASEB

Annals of Biomedical Engineering, Vol. 33, No. 5, May 2005 (© 2005) pp. 696–708
DOI: 10.1007/s10439-005-1690-5

Coordinated Movement of Bile Canalicular Networks Reconstructed by Rat Small Hepatocytes

RYO SUDO,[1] HIROSHI KOHARA,[1] TOSHIHIRO MITAKA,[2] MARIKO IKEDA,[1] and KAZUO TANISHITA[1]

[1]Center for Life Science and Technology, School of Fundamental Science and Technology, Keio University, Yokohama, Kanagawa 223-8522, Japan and [2]Department of Pathophysiology, Cancer Research Institute, Sapporo Medical University School of Medicine, Sapporo, Hokkaido 060-8556, Japan

(Received 6 March 2004; accepted 1 December 2004)

Abstract—Hepatocytes *in vivo* have a potential for liver regeneration, but it has been very difficult to reconstruct hepatic organoids *in vitro*. Recent studies have shown that small hepatocytes (SHs) can reconstruct hepatic organoids including functional bile canaliculi (BC). In the present study we analyzed the movement of BC formed in the hepatic organoids, focusing on the coordination of contraction and dilation among cells and the mechanism producing the coordination. Hepatic cells, including SHs, were isolated from an adult rat liver and cultured. Time-lapse images of BC movements were taken and analyzed in cells treated with or without cytochalasin B (CB). Time-lapse images revealed that all BC, regardless of region contracted in a coordinated manner. Actin filaments were observed along the BC even after the BC networks treated with CB dilated markedly. Microinjection of dye was also carried out to investigate the flow thorough BC. Secreted fluorescein from the injected cell flowed along BC, and gap junctional protein connexin 32 was expressed along BC networks, suggesting cell-to-cell communication. Thus, groups of hepatocytes in the hepatic organoids act in a coordinated manner through intercellular communication.

Keywords—Gap junctional communication, Actin, Cytochalasin B.

INTRODUCTION

Liver regeneration is a unique capability of the liver *in vivo*.[5,16] It is well known that hepatocytes can proliferate to recover the lost tissue after two-thirds partial hepatectomy. Although hepatocytes *in vivo* have the potential for liver regeneration, it has been very difficult to reconstruct hepatic tissues *in vitro*. However, reconstruction of hepatic organoids is needed for the transplantation of tissue-engineered organs.[37]

Recently, two approaches for the culture of hepatic organoids have been demonstrated.[15,20] Hepatic progenitor cells, identified as proliferating cells with hepatic characteristics, were found and named small hepatocytes (SHs).[17,18,21] Although primary hepatocytes rapidly lose their function with time in culture, SHs can reconstruct hepatic organoids interacting with hepatic nonparenchymal cells (NPCs) such as liver epithelial cells and stellate cells.[20] For hepatic organoid formation, extracellular matrices, especially components of basement membrane such as laminin and type IV collagen, were shown to be important and treatment with EHS gel (Matrigel®) could induce the maturation of SHs.[36] On the other hand, Michalopoulos *et al.*[15] reported that they developed hepatic organoids consisting of hepatocytes and fenestrated endothelium when hepatic cells on polystyrene beads were cultured in roller bottles. Furthermore, when cells isolated from a rat liver were cultured in the roller bottles with rotation, the cells formed a characteristic and reproducible tissue architecture composed of a superficial layer of biliary epithelial cells, an intermediate layer of connective tissue and hepatocytes, and a basal layer of endothelial cells.[14] These experiments demonstrated the formation of hepatic organoids, and revealed the structural features of the organoids. Although the formation of hepatic organoids has been morphologically investigated, tissue-level functions of the cells are not well analyzed.

Bile canalicular contraction is one of the tissue-level functions of the liver, because it is achieved by the coordination of adjacent hepatocytes. Bile canaliculi (BC) are tubular structures that form the most proximal channels of the biliary tree and carry bile secreted by hepatocytes. To expel bile through BC, a series of hepatocytes along BC must contract in a coordinated fashion. Therefore, the hepatic tissue needs to have communications and integration among neighboring hepatocytes.

Address correspondence to Ryo Sudo, Center for Life Science and Technology, School of Fundamental Science and Technology, Keio University, 3-14-1 Hiyoshi, Kohoku-ku, Yokohama 223-8522, Japan. Electronic mail: sudo@tani.sd.keio.ac.jp

Abbreviations: SH, small hepatocyte; BC, bile canaliculi; CB, cytochalasin B; NPC, nonparenchymal cell; Cx, connexin; ROI, region of interest; FD, fluorescein diacetate; DAPI, 4′, 6-diamidino-2-phenylindole; CMFDA, CellTracker™ green 5-chloromethyl-fluorescein diacetate; MRP2, multidrug-resistance associated protein 2.

It has been difficult to reconstruct hepatic organoids possessing BC networks with motile activity. However, we recently demonstrated that SHs could form BC with motility and secretory function.[35] BC were formed and three-dimensionally extended BC networks were developed in the hepatic organoids. In the reconstructed tissues, BC could continuously contract and dilate. Although the motility of BC was demonstrated, coordination of the movements was not analyzed. To understand the mechanism of bile transportation, the coordination of BC movements should be clarified. Thus, in the present study we analyzed movements of BC formed in the hepatic organoids and verified that BC movements were coordinated. We found that BC contractions occurring in different regions could act synchronously, and that intercellular communication through gap junctions might be important for the coordination of BC movements.

MATERIALS AND METHODS

Isolation and Culture of SHs and NPCs of the Rat

The cells were isolated from male Sprague-Dawley rats (250–450 g; Nippon Bio-Supp. Center, Tokyo, Japan) using Seglen's[32] two-step liver perfusion method with some modifications.[20] All animals used in the experiments received humane care and the experimental protocol was approved by the Committee of Laboratory Animals following Keio University guidelines. Details of isolation and culture of liver cells were previously described.[20] The cells were suspended in DMEM (Sigma-Aldrich Co., St. Louis, MO) with 20 mM HEPES, 25 mM $NaHCO_3$, 30 mg/l L-proline, 0.5 mg/l insulin, 10^{-7} M dexamethasone, 10% FBS, 10 mM nicotinamide (Sigma-Aldrich), 1 mM ascorbic acid 2-phosphate (Wako Pure Chemical, Tokyo, Japan), 10 ng/ml EGF (BD biosciences, Bedford, MA) and antibiotics, and the number of viable cells was counted. The cells were inoculated on culture dishes (4.5×10^5 viable cells/35-mm dish; Corning Glass Works, Corning, NY) coated with rat-tail collagen (50 μg of dried tendon/0.1% acetic acid) and placed in a humidified, 5% CO_2/95% air incubator at 37°C. Medium was changed to remove dead cells about 3 h after inoculation, and the medium was subsequently changed every other day. After day 4 (96 h after plating), 1% DMSO (Sigma-Aldrich) was added to the culture medium.

Time-Lapse Microscopy for the BC Contractions

Cells were placed in a humidified 5% CO_2/95% air chamber (Sankei Co., Tokyo, Japan) at 37°C, and photographed using a phase-contrast microscope (TE300; Nikon, Tokyo, Japan) equipped with a CCD camera (Roper Scientific, Trenton, NJ). Images of the BC networks formed in a colony with piled-up cells were recorded at 5-s intervals for 3 h. The sequential images (2,160 frames/colony and 17 colonies) were analyzed using the MetaMorph® imaging system (Universal Imaging Corporation™, Downingtown, PA).

Analysis of BC Movements

In this experiment, 17 colonies including well-developed BC networks were photographed using a phase-contrast microscope equipped with a time-lapse device. Measurement of BC movements was based on variations of translucent areas coinciding with BC networks in the sequence of phase-contrast micrographs. To quantify the BC areas, a specific threshold value that distinguished BC from cytoplasm was chosen with reference to translucent belts seen under phase-contrast microscopy. The threshold value was set using the first image of the time-lapse series because pixel intensity of the translucent belts varied in each time-lapse series. The threshold value was adjusted to fit thresholding areas to the translucent belts. For the quantitative analysis of the BC movement in the time-lapse series, thresholding was applied to the first time-lapse image and the same threshold value of the light intensity was applied to the other sequential images so that consistent thresholding applied. Next, four regions of interest (ROIs) were set for each image in the time-lapse series. To investigate the movements of various parts of the BC network, ROIs were randomly placed throughout the colony in the first image, avoiding neighboring cells. The same ROIs were set in the other sequential images of the same time-lapse series. We then measured the thresholding areas within each ROI to investigate the width of each BC. The thresholding areas were normalized by dividing the measurement of each time by that of the initial time. Variations of the normalized thresholding areas were compared to analyze the BC movements. Therefore, the results accurately represent BC movements without any biased data. The variations in the thresholding areas reflect the width of the BC. In this experiment, BC in 68 ROIs (4 ROIs/colony and 17 colonies) were analyzed.

To quantify the coordination of BC movements, a correlation coefficient was calculated for each colony. The correlation coefficients between the values of each ROI during the observation period (10 min for fast movements, 30 min for slow movements) were calculated. The correlation coefficient R_{xy} between pairs of the thresholding area in each ROI is given as

$$R_{xy} \frac{\sum (x_i - \bar{x})(y_i - \bar{y})}{\sqrt{\sum (x_i - \bar{x})^2 \sum (y_i - \bar{y})^2}} \quad (1)$$

where $\bar{x}$ and $\bar{y}$ are mean thresholding areas in each ROI. R_{xy} ranges from -1 to $+1$, and -1 and $+1$ show strong associations in a negative and positive manner, respectively.

FD Treatment

In hepatocytes, fluorescein diacetate (FD) is metabolized by intracellular esterase, to become fluorescein. The

cytoplasmic fluorescein is actively transported into the BC via multidrug-resistance associated protein 2 (MRP2). To visualize the lumen of the BC networks, FD was added to the medium at a final concentration of 2.5 μg/ml. After 15-min incubation, the cells were rinsed three times with a medium containing no FD and then photographed using a phase-contrast microscope equipped with a fluorescence device.

CB Treatment and Immunocytochemistry for Actin

To investigate the effects of cytochalasin B (CB; Sigma-Aldrich) on the behavior of BC networks, SH colonies were treated with CB. Sequential photographs were taken soon after the addition of CB to the medium. The CB solution was prepared from stock solution (25 mg/ml in DMSO). The cells were treated with a final concentration of 0.1, 1.0, 5.0, and 10.0 μg/ml CB in modified DMEM for 3 h. After images were obtained, the cells were fixed in cold absolute ethanol and kept at −20°C until use. The actin filaments were visualized by incubation with Alexa Fluor 594 phalloidin (Molecular Probes, Eugene, OR) for 1 h.

Immunofluorescent Staining for Gap Junctional Protein Cx 32

The cells cultured on coverslips coated with rat-tail collagen were fixed in cold acetone for 5 min and double-immunofluorescent staining for connexin 32 (Cx 32) and actin was carried out. We used a mouse anti-Cx 32 antibody (Zymed Laboratories Inc., South San Francisco, CA) as the primary antibody and Alexa Fluor 594 phalloidin (Molecular Probes). An Alexa Fluor 488 anti-mouse IgG antibody (Molecular Probes) was used as the secondary antibody. The dishes were mounted with 90% glycerol containing 1 g/l *p*-phenylenediamine and 1 mg/l 4′, 6-diamidino-2-phenylindole (DAPI; Sigma-Aldrich).

Microinjection of Dye into the Piled-Up Cells and Transportation of Fluorescence

Before dye microinjection, the medium was replaced with L-15 (Invitrogen Co., Grand Island NY) medium. To observe flow through BC, 10 μM CellTracker™ green 5-chloromethyl-fluorescein diacetate (CMFDA; Molecular Probes) was microinjected (Eppendorf Micromanipulator system; Eppendorf, Hamburg, Germany) into one of the piled-up cells in each colony. When CMFDA is microinjected into cells, esterase in their cytoplasm hydrolyzes nonfluorescent CMFDA to fluorescent 5-chloromethylfluorescein. In hepatocytes, ATP-dependent multidrug transporters excrete the glutathione-conjugated fluorescent dye into BC.[30] Fluorescent images of the cells were recorded at 5-s intervals for 5 min using a fluorescence microscope equipped with a time-lapse system (Roper Scientific). More than 10 microinjections were performed.

RESULTS

BC Formation and Quantification of the BC Area

SHs started to proliferate 2–3 days after inoculation and then formed colonies. Although SH colonies appeared as flat clusters in the early period of the culture, they expanded to form large colonies, some of which were composed of piled-up cells. The piled-up cells had the appearance of mature hepatocytes. In the areas between the piled-up cells BC formed and developed into anastomosing networks as we previously reported.[35] One-fourth of the SH colonies displayed the piled-up cells that formed BC by day 30.[19]

BC networks were detected as translucent belts under phase-contrast microscopy [Fig. 1(A)]. We ascertained whether the translucent belts represented the width of the BC using FD as a probe to visualize BC networks. The BC in the piled-up SHs are functional as an apical domain including the secretory functions for bilirubin and fluorescein as we previously reported.[35] In addition, secreted fluorescein was not diffused after rinsing with the medium because the BC were sealed by tight junctions as previously reported by immunocytochemistry for tight junction-associated protein ZO-1.[35] Therefore, secreted fluorescein can indicate the

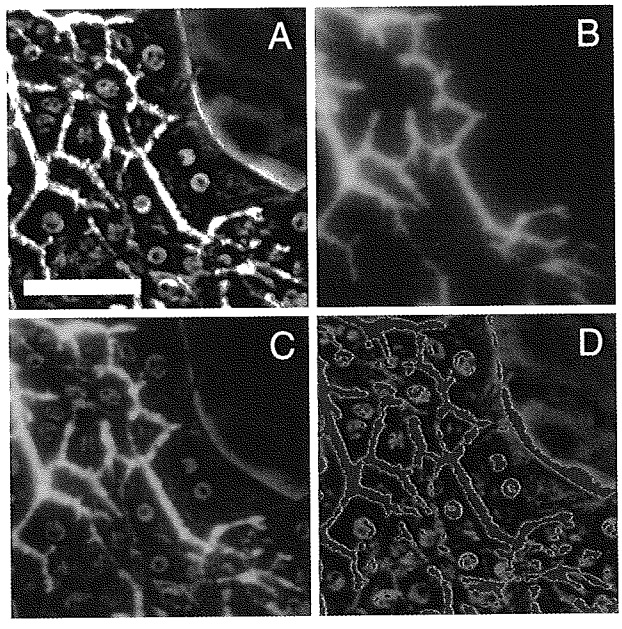

FIGURE 1. Corresponding images of an SH colony in which piled-up cells formed BC networks. A: phase-contrast micrograph of the cells at day 30 shows translucent networks between the cells representing BC. B: fluorescent image of the cells after FD treatment shows metabolized fluorescein secreted into BC. C: the merged image of the phase-contrast and fluorescent image indicates that the translucent networks under phase-contrast microscopy coincide with the fluorescent networks of fluorescein. D: the merged image of the phase-contrast and thresholding images. Thresholding to the phase-contrast image was applied to clarify the region of the BC, and is shown in red. Scale bar, 50 μm.

width of the BC. The fluorescent intensity in intercellular spaces was detected after FD treatment [Fig. 1(B)]. The fluorescein localized in the restricted areas of intercellular spaces that represented BC networks. Under phase-contrast microscopy, the merged images showed translucent belts that coincided with fluorescent networks [Fig. 1(C)]. These results suggested that the translucent belts observed under phase-contrast microscopy corresponded exactly to the width of the BC. Therefore, BC movements were analyzed based on variations in the translucent areas under phase-contrast microscopy. In order to quantify the translucent areas, thresholding was applied to phase-contrast micrographs to coincide with the translucent belts [Fig. 1(D)]. This thresholding was feasible because the thresholding images [red area, Fig. 1(D)] corresponded to the fluorescent images [green area, Fig. 1B)].

BC Movements in the Piled-Up Colonies

Time-lapse microscopy revealed that BC movements occurred in the piled-up cells. Figure 2 shows an SH colony composed of the piled-up cells that form the BC. In the region indicated with rectangle *a* in Fig. 2(A), the left BC contracted in the early period of the experiment [left arrowheads, Figs. 2(B) and (D)]. The right BC contracted next [right arrowheads, Figs. 2(D) and (F)]. On the other hand, BC in rectangle *b* remained wide or dilated while the BC in rectangle *a* contracted [arrowheads, Figs. 2(C), (E), (G), (I)]. In addition, the cystic structure that formed in the tip of the colony [asterisk, Fig. 2(A)] dilated following the BC contraction in rectangle *a* and the dilation in rectangle *b* (data not shown). These sequential movements of BC suggested a flow of the fluid toward the cystic structure.

Some BC contractions were synchronized (Fig. 3). BC in the top rectangle [rectangle, Fig. 3(A)] contracted synchronously when the BC in the lower rectangle [rectangle, Fig. 3(A)] contracted (arrowheads, Figs. 3(C–F)). To clarify this phenomenon, the BC movements were analyzed using the thresholding methods. The thresholding was applied to each image of the time-lapse series and ROIs were set on each image [a, b, Fig. 3(B)]. Variations of the normalized thresholding areas within each ROI are graphically shown in Fig. 3(G). The BC contraction that was observed in the time-lapse images was consistent with the variations of the normalized thresholding area in the graph [between 82 min and 107 min, Fig. 3(G)]. The maximum amplitude of each graph [amp, Fig. 3(G)], which indicates the degree of the BC movement in each ROI, was calculated by subtracting the minimum value [min, Fig. 3(G)] from the maximum value [max, Fig. 3(G)] in the experimental period.

In the present experiment we analyzed 68 ROIs of BC in 17 colonies. Some BC dramatically contracted or dilated, others showed small morphological changes. Each BC had its own motility, which was represented by a maximum amplitude. To show the motility of the BC, the maximum

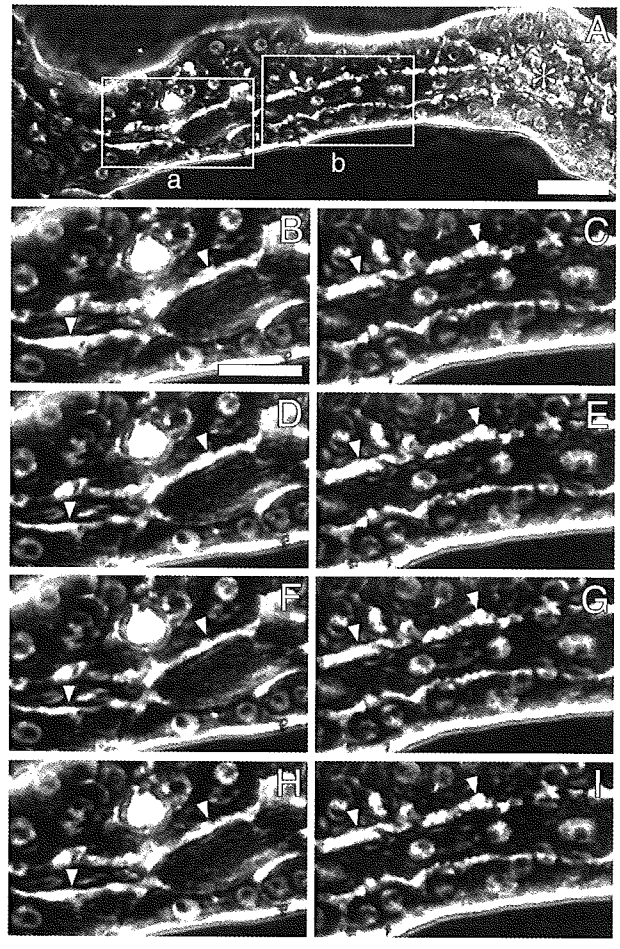

FIGURE 2. Phase-contrast micrographs of the cells that form BC. A: Parallel BC developed in the piled-up cells at day 27. B–I: Enlarged time-lapse images of the same part indicated by the rectangle *a* (B, D, F, H) and *b* (C, E, G, I) in A. The total number of the time-lapse images was 2160. The frame numbers are 75 (B, C), 79 (D, E), 82 (F, G), and 100 (H, I), respectively. BC contractions were detected in the sequential images (arrowheads). Scale bars, 50 μm (A) and 30 μm (B).

amplitude of each BC movement was calculated and represented in the form of a histogram (Fig. 4). The maximum amplitude had a wide range, varying from 0.2 to 1.8, and no frequency at the range of 0.0–0.2. These results indicate that the BC of each colony had various kinds of motility, and all BC had motility of at least 0.2 in the experimental period. In addition, the most probable motility was in the range of 0.4–0.6 (Fig. 4), which suggests the area was increased or decreased by 40–60% when compared with the initial BC area.

Coordination of the BC Movements

Analysis of the time-lapse images showed that coordination of BC contractions and dilations appeared to be present. We classified BC movements according to the speed of movement: BC movements within 10 min (fast)

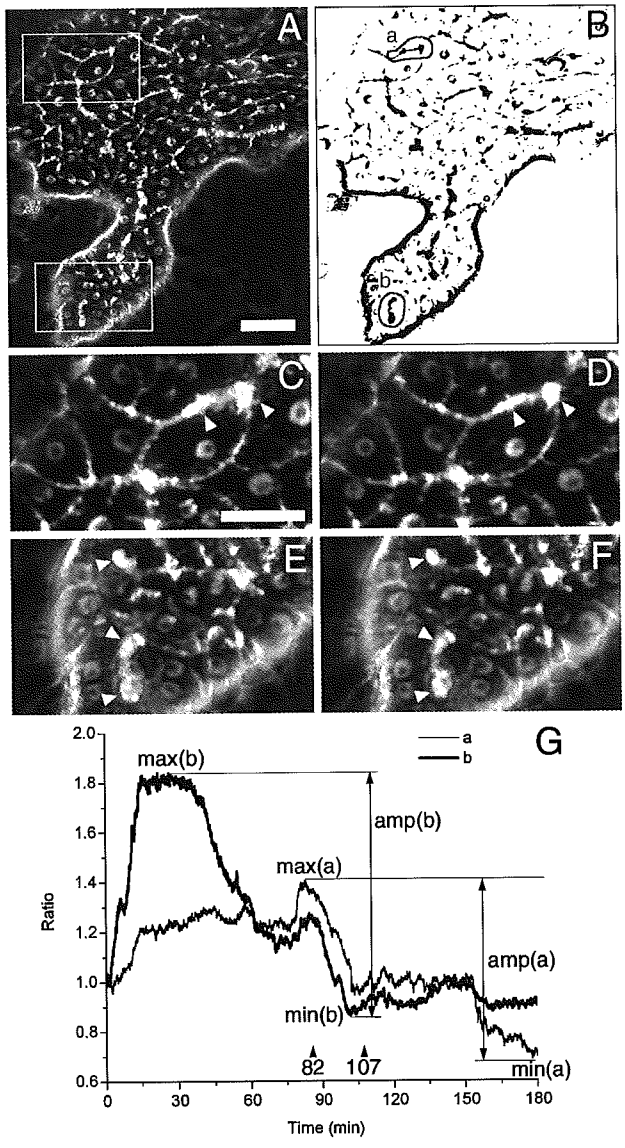

FIGURE 3. Phase-contrast micrographs and graphical representation of BC movements. A: Phase-contrast micrograph of the piled-up cells at day 23. B: Thresholding was applied to A. ROIs were set on the image (a, b). C–F: Enlarged images of the same parts indicated by rectangles in A (top rectangle: C–D, lower rectangle: E–F). Images correspond to the times of 82 min (C, E) and 107 min (D, F), indicated by arrowheads in G. G: Graphical representation of BC movements in two ROIs (a, b, B). The thresholding area within the ROIs of each time was calculated and the values were normalized by dividing each value by the initial value. Maximum amplitude of each graph is shown by vertical arrows designated amp (a) and amp (b). Scale Bars, 50 μm (A) and 30 μm (C).

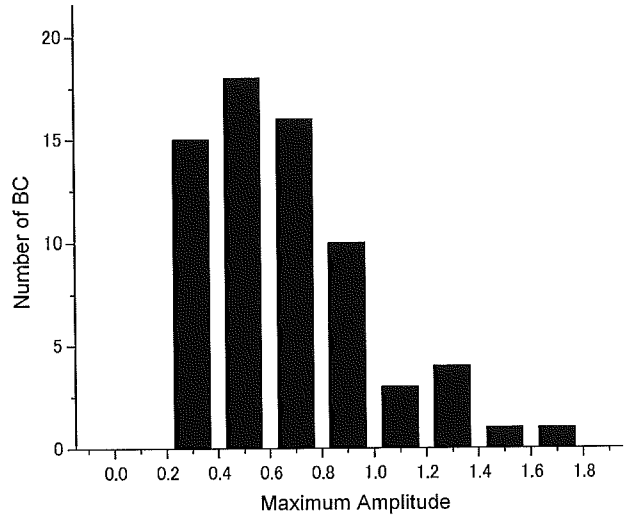

FIGURE 4. Maximum amplitude histogram of the total BC in ROI. In this experiment, 68 regions of BC (4 ROIs/colony and 17 colonies) were analyzed and the maximum amplitude of the graph in the experimental period (3 h) was measured. Note that there is a peak at the maximum amplitude of 0.4–0.6. There is no frequency at the maximum amplitude of 0.0–0.2.

and those that continued for more than 30 min (slow). We also classified BC movements according to whether the movements were coordinated or not. Visual analysis of the movie showed that all colonies had BC movements, and 94% of those were coordinated (Table 1).

By further observation of time-lapse images, we found that BC movements could be classified into three types. Therefore, we show three typical types of BC movement in Fig. 5 although 17 colonies were analyzed. Figure 5 shows BC movements in three colonies in which different types of movement occurred. BC dramatically contracted and dilated as shown in Figs. 5(C), (F), and (I), and coordination of movements was observed. The coordination was observed in the contractions of both fast and slow types and the observation periods are indicated by the closed box [p1–9, Figs. 5(C), (F), (I)]. For quantitative analysis of the coordination, we calculated correlation coefficients during periods p1–9, and the values are shown in Table 2. Thus, Fig. 5 shows the BC movements and the values in Table 2 show the degree of the coordination corresponding to Fig. 5. In this study, BC movements with an absolute correlation coefficient value of more than 0.66, the average value, were presumed to be coordinated. At least one correlation coefficient between the ROIs was more than 0.66 in all periods (asterisks, Table 2), which indicates that BC movements occurring in neighboring areas were coordinated. (1) Figures 5(A–C) show the BC movements which occurred throughout the colony. There were three contractions in the experimental period [arrowheads, Fig. 5(C)]. Figure 5(C) and Table 2 show that in the contraction in period p1 [p1, Fig. 5(C)], the values of the correlation coefficients between #1–#4, #2–#3, #2–#4, and #3–#4 were 0.67, 0.93, 0.96, and 0.97, respectively (p1, Table 2). Similarly, in the contractions at periods p2 and p4 the correlation coefficients between each ROI were more than 0.86 (p2, p4, Table 2). Thus, although the BC in region #1 was about 10 cells distant from that in region #4, BC around the areas including #1, #2, #3, and #4 were synchronously moving. (2)

TABLE 1. Motilities of the BC networks in SH colonies

	Fast		Slow		
	Contraction	Dilatation	Contraction	Dilatation	Either
Movement	10 (59%)	3 (18%)	11 (65%)	16 (94%)	17 (100%)
Coordination	9 (53%)	3 (18%)	8 (47%)	9 (53%)	16 (94%)

Note. Each value indicates the number of colonies in which BC movements (upper) or coordinated movements (lower) occurred in the experimental period. Percentages are in brackets. BC movements of 17 colonies were classified into two types depending on the rate of movement, BC movements within 10 min (fast) and those of more than 30 min (slow).

Figures 5(D–F) show the BC movements, speed of which was relatively fast, and cellular contraction can be observed. The correlation coefficients at periods p5 and p6 showed negative values, proving the BC dilations (#4) were followed by a BC contraction (#1) in the neighboring area (p5–6, Table 2). (3) Figures 5(G–I) show the BC movements, the speed of which was relatively slow. The correlation coefficient between #1–#3 at the period p8 was positive, while that at the period p9 was negative (p8–9, Table 2). These results indicated that BC both in #1 and #3 dilated at period p8, although the BC in #1 contracted at period p9 while BC in #3 dilated.

CB Treatment

CB inhibits polymerization of actin by binding to the barbed ends of actin filaments.[2,4,6] The agent has been widely used to study the role of actin in biological processes.[4] Numerous actin filaments have been observed around the BC in hepatocytes, which suggests that they play an important role in BC contraction.[29] Therefore, the role of actin in BC contraction was studied using CB.

As shown in Fig. 6, the morphology of BC in piled-up cells treated with CB dramatically changed. The BC started to dilate soon after the addition of CB. When the cells were treated with 1.0 μg/ml CB, BC became progressively dilated for 1 h, and then maintained that width for more than 2 h [Figs. 6(A–C)]. On the other hand, when the cells were treated with 5.0 μg/ml CB, BC became progressively dilated throughout the experimental period, and cystic structures were observed [arrowheads, Fig. 6(F) inset]. Cystic dilation of BC was noticeable near the edges of the colony. Remarkable dilations of the BC network were observed at 60 min after addition of CB [Fig. 6(E)], and canalicular structures changed into cystic ones after 180 min [Fig. 6(F)]. The motility of BC was reduced, and no contraction was observed when the cells were treated with CB at concentrations of more than 1.0 μg/ml. In contrast, when the cells were treated with low concentration (0.1 μg/ml) of CB, no remarkable dilatations of BC were observed (data not shown).

As shown in Fig. 7, actin filaments were abundant around BC in the cells treated with each concentration of CB. The actin filaments around the BC revealed narrow spaces between them in cells without CB treatment [arrowheads, Fig. 7(A)]. On the other hand, when the cells were treated with 1.0 μg/ml CB, the actin filaments around the BC were wider [arrowheads, Fig. 7(B)]. In addition, when the cells were treated with a high concentration (5.0 μg/ml) of CB, the actin filaments showed indented distribution around the dilated BC [Fig. 7(C)]. Some actin filaments were also distributed in the cytoplasm [asterisks, Fig. 7(C)], and increased intensity of positivity was heterogeneously observed along the BC [arrowheads, Fig. 7(C)].

Immunocytochemistry for Cx 32

Immunocytochemistry for Cx 32 was carried out to determine whether the piled-up cells had the ability to communicate via gap junctions. Immunocytochemistry for actin was also carried out to visualize cell–cell borders. Actin in the piled-up cells was intensively stained around the BC [inset, Fig. 8(C)]. Cortical actin was observed in those SHs that form no BC between the cells [inset, Fig. 8(G)]. Dotted expression of Cx 32 was distributed on basolateral membranes that coincided with the translucent belts formed in the piled-up cells, although the expression had heterogeneity [Figs. 8(A–D)]. By contrast, no Cx 32 was expressed in the cytoplasm of the flat cells and no localization was observed [Figs. 8(E–H)].

Secretion of Microinjected Dye in Piled-Up Cells

CMFDA was microinjected into one of the piled-up cells in the colony [asterisk, Fig. 9(A)]. It was metabolized within the injected cell and the metabolite was excreted into BC by a transporter such as MRP2. As previously reported, MRP2 is uniformly expressed on BC membranes of the piled-up cells.[35] As shown in Fig. 9(C), soon after the injection bright fluorescence was observed in the cytoplasm of the cell and a line of fluorescence extended in the direction of the tip of the colony. Two and half minutes later, the dye was clearly detected in four cells distant from the injected cell [arrowhead,

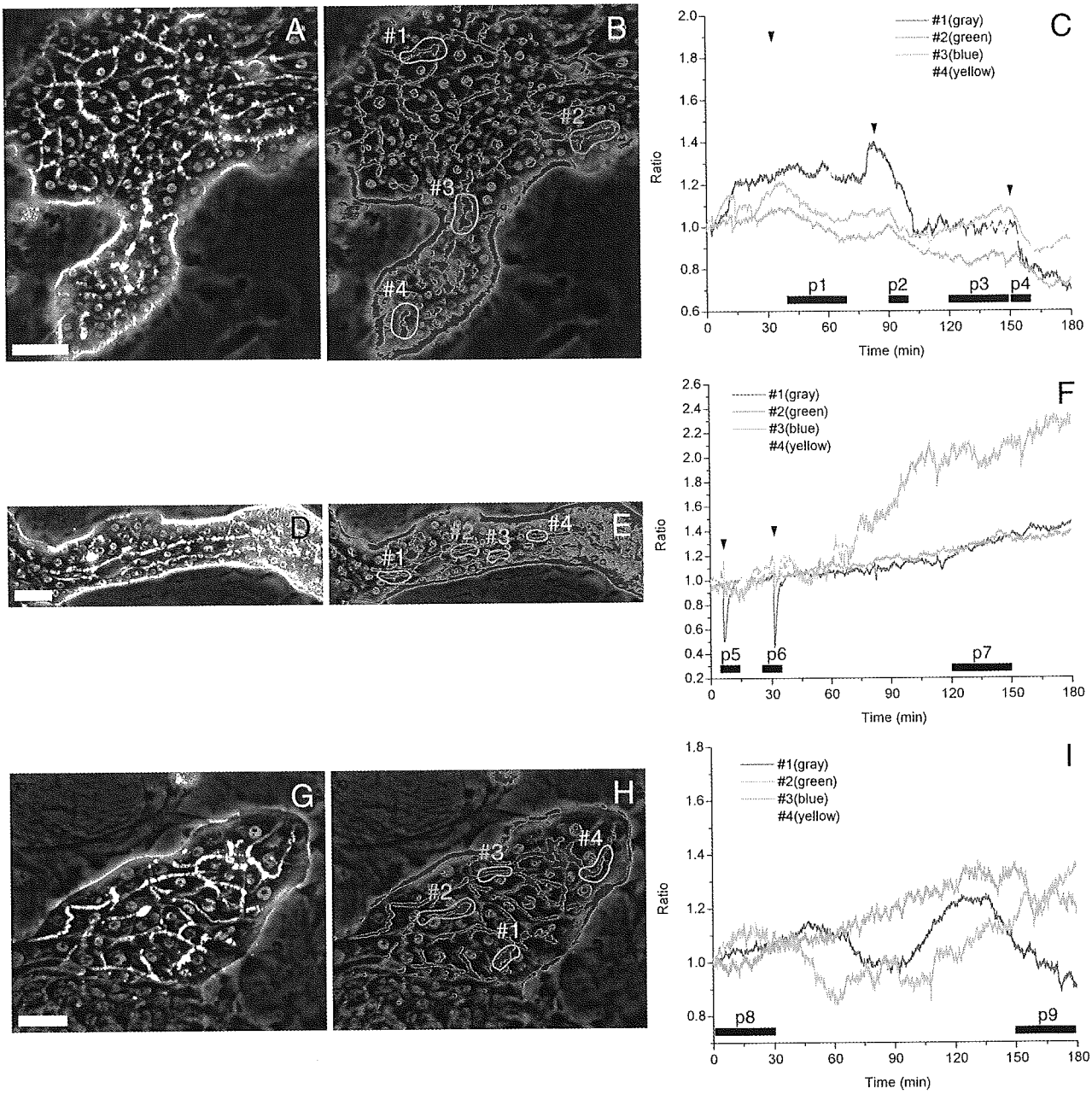

FIGURE 5. Corresponding phase-contrast (A, D, G), thresholding images (B, E, H) and graphs (C, F, I). Thresholding was applied to phase-contrast images of the piled-up cells at A: day 23, D: day 27, and G: day23, and B, E, H: the merged images of each phase-contrast and thresholding image are shown. C, F, I: The graphs indicate the variations of the thresholding area in each ROI set on the thresholding image (#1–4, B, E, H), normalized by division by the value at the initial time in the experimental period. Closed boxes (p1–9, C, F, I) indicate observation periods in which correlation coefficients were calculated. Arrowheads indicate contractions. Scale bars, 50 μm (A, D, G).

Fig. 9(E)]. The intensity was observed within BC branching toward the tip of the colony. In the piled-up cells, Cx 32 was expressed along the BC. Therefore, the dye might have been transferred through gap junctions although cells adjacent to the injected one were only faintly stained. The fluorescence intensity increased in the route of the transferred dye for several minutes and then gradually decreased.

DISCUSSION

Coordination of BC Contraction

The BC form a pathway to transport bile secreted by hepatocytes. Transportation of bile is very important because disorders of bile transportation are associated with cholestasis. Therefore, motility of BC is necessary for the

TABLE 2. Correlation coefficients between BC movements in different ROIs

		#1	#2	#3	#4
p1	#1	1.00			
	#2	0.65	1.00		
	#3	0.61	0.93*	1.00	
	#4	0.67*	0.96*	0.97*	1.00
p2	#1	1.00			
	#2	0.93*	1.00		
	#3	0.88*	0.92*	1.00	
	#4	0.96*	0.95*	0.94*	1.00
p3	#1	1.00			
	#2	0.12	1.00		
	#3	−0.15	0.41	1.00	
	#4	−0.17	0.47	0.92*	1.00
p4	#1	1.00			
	#2	0.90*	1.00		
	#3	0.95*	0.88*	1.00	
	#4	0.96*	0.86*	0.95*	1.00
p5	#1	1.00			
	#2	0.43	1.00		
	#3	−0.19	−0.47	1.00	
	#4	−0.67*	−0.16	−0.24	1.00
p6	#1	1.00			
	#2	0.95*	1.00		
	#3	0.35	0.26	1.00	
	#4	−0.89*	−0.92*	−0.13	1.00
p7	#1	1.00			
	#2	0.83*	1.00		
	#3	0.02	0.04	1.00	
	#4	0.85*	0.86*	0.06	1.00
p8	#1	1.00			
	#2	0.50	1.00		
	#3	0.61	0.06	1.00	
	#4	0.74*	0.70*	0.40	1.00
p9	#1	1.00			
	#2	0.41	1.00		
	#3	−0.75*	−0.27	1.00	
	#4	0.69*	0.57	−0.40	1.00

Note. Correlation coefficients between pairs of thresholding areas in each ROI (#1–4, Figs. 5B, E, H) during periods indicated by a closed box (p1–9, Figs. 5C, F, I) were calculated. Coefficients whose absolute values were more than 0.66 are presumed to be coordinated (asterisks).

physiological function. In addition, coordination of BC movements is sequential and synchronous, and therefore essential for transporting bile into bile ducts. BC contractions were first observed in hepatocyte couplets, intact pairs of hepatocytes isolated from rat livers.[26] Subsequent studies using couplets demonstrated BC contractions,[27,34] the Ca^{2+}-induced BC contractions,[43] and some agents to increase the BC contractions.[8,22,45] Although hepatocyte couplets are useful models for analysis of BC contractions, coordination of adjacent hepatocytes along BC could not be investigated because BC in couplets form a closed sphere, whereas the BC *in vivo* form a tubular structure. BC movements and the coordination of these movements have not been investigated in studies that investigated BC formation using the collagen gel sandwich method[12,38] and hepatocyte spheroid culture.[10,11] Therefore, this BC network made it possible to analyze the coordination of the SHs required for tissue-level function.

In the present experiment we analyzed BC movements to determine whether they were coordinated. Time-lapse microscopy revealed sequential contraction along the BC (Fig. 2) and coordination of BC contraction (Fig. 5). The degree of the coordination was quantified to calculate the correlation coefficient. Although each BC had its own motility (Fig. 4), the values of the correlation coefficients during the observed periods (p1–9, Fig. 5) were more than 0.66, which suggests coordination of the BC contraction (Fig. 5, Table 2). These results suggest that individual cells forming BC act in a coordinated manner to achieve an integrated function for the transportation of bile.

Intercellular Communication for the Coordination

Various intracellular processes in the liver are known to be coordinated by second messengers such as cAMP, cytosolic Ca^{2+}, and inositol trisphosphate.[3,7,31,39,44] An organ-level response to hormonal stimuli may be produced by integration of signals among hepatocytes within the liver plate.[23,24,40] Nathanson *et al.*[25] reported that the organization of second messenger signals across the hepatic lobule played an important role in hormonal regulation of bile secretion in the perfused liver. Serriere *et al.*[33] reported that unidirectional agonist-induced intercellular Ca^{2+} waves via gap junctions might drive canalicular peristalsis and increase bile flow.

To reconstruct hepatic tissues, proliferation and interaction of SHs and NPCs are essential. It has been reported that hepatocytes can maintain viability for extended periods when the cells form three-dimensional aggregates like spheroids.[10,11] Although the hepatocytes in spheroids could express differentiated functions and form BC-like structures, apical domains of these cells were gradually lost with time in culture.[1] On the other hand, after SHs proliferate and form colonies within a couple of weeks, matured SHs appear on the colonies, in which BC networks are well developed.

In the present experiment we investigated the cellular ability for the intercellular communication to immunostain gap junctional protein Cx 32. The piled-up cells expressed Cx 32 in the basolateral membranes along BC networks although no expression of Cx 32 in the basolateral membranes was observed in the proliferating SHs that were not mature and formed no BC (Fig. 8). Cx 32 was expressed heterogeneously along BC networks (Fig. 8), which suggested the heterogeneity of BC movements. BC networks started to form in piled-up colonies. As these piled-up areas developed in the colony, the networks gradually expanded. Thus, considering the temporal formation of the BC, BC networks in piled-up colonies might be heterogenous. In

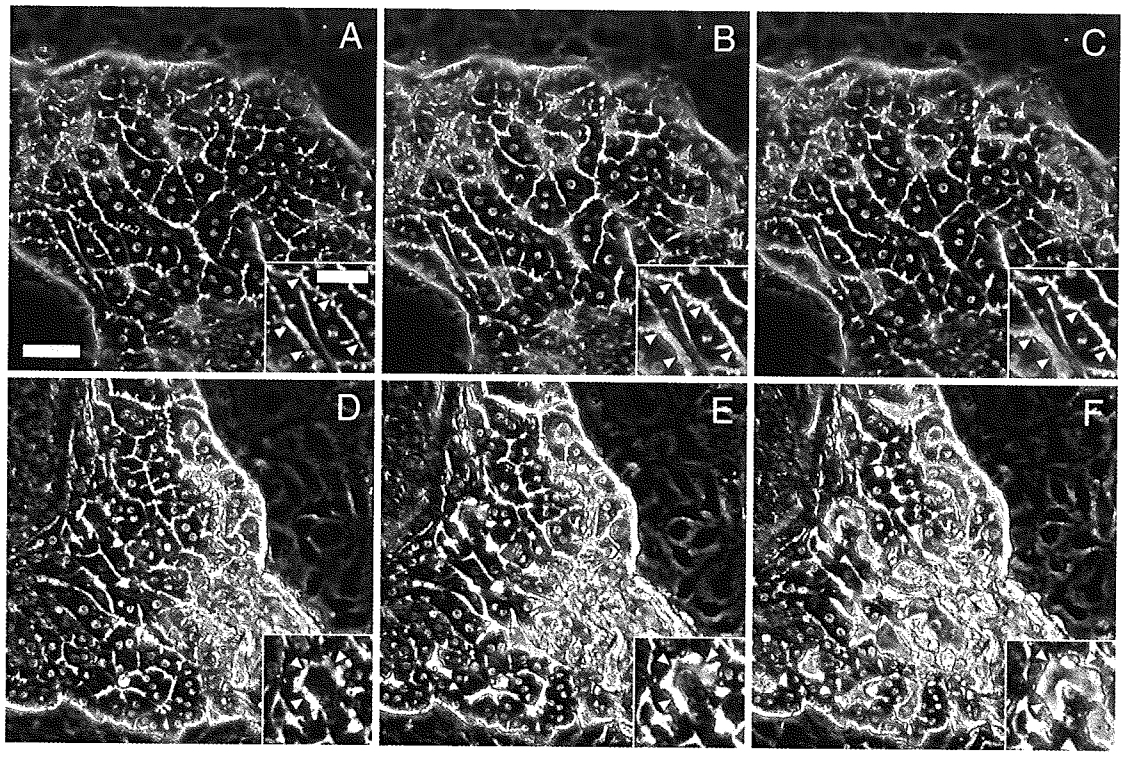

FIGURE 6. Time series phase-contrast images of the cells reconstructing BC networks at day 43 under administration of CB (1.0 μg/ml: A–C, and 5.0 μg/ml: D–F). Corresponding images of the cells after administration of CB shows dilation of BC networks. A, D: immediately after administration, B, E: after 60 min, C, F: after 180 min. Insets in each figure show magnified images of corresponding BC (arrowheads, A–F insets). Scale bars, 50 μm (A), and 30 μm (A inset).

addition, analysis of the BC movements revealed that even within a colony there were regions where the BC could act in a coordinated fashion, which was also consistent with the heterogenous expression of Cx 32. Furthermore, treatment with A23187, a Ca^{2+} ionophore, transiently induced coordinated BC contraction (data not shown). Thus, coordination of neighboring and apposing SHs may integrate the action of the whole BC network by second messengers such as Ca^{2+} and inositol trisphosphate via gap junctions.

The Role of Actin in BC Contraction

The role of actin in BC contraction has been investigated using CB. When CB is administered to rats, dilated BC are visualized in the liver.[46] The dilation is also observed in

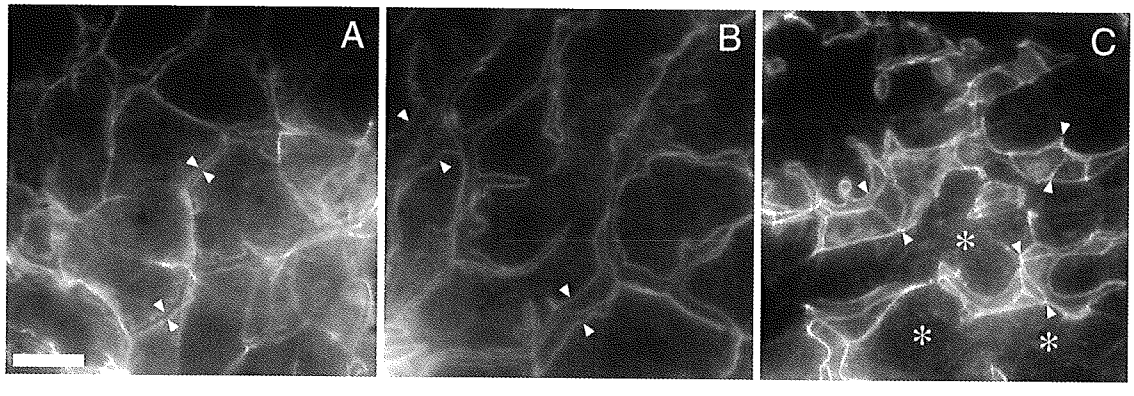

FIGURE 7. The localization of actin filaments in the piled-up cells reconstructing BC networks at day 43. A: the control cells show intensive expression of actin filaments around BC (arrowheads). B: administration of 1.0 μg/ml CB causes wide spaces between actin filaments coinciding with dilation of BC (arrowheads). C: the actin filaments of the cells treated with 5.0 μg/ml CB show indented distribution around dilated BC (arrowheads). In addition, dotted intensities in the cytoplasm (asterisks) and heterogeneity of the intensity around BC are observed.

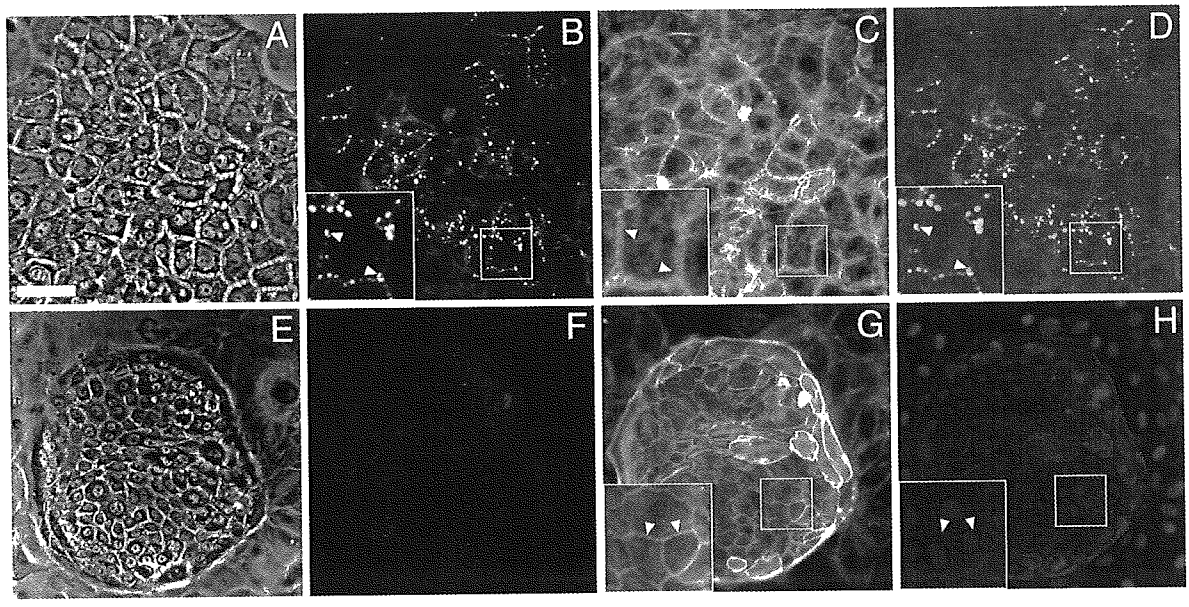

FIGURE 8. The localization of Cx 32 protein in the flat cells and piled-up cells reconstructing BC. Triple immunostaining for Cx 32 (green), actin (red), and DAPI (blue) was carried out. Phase-contrast micrographs of the cells at day 27 (A) and day 26 (E). Corresponding images of Cx 32 (B, F), actin (C, G), and the merged images of Cx 32, actin and DAPI (D, H). Dotted expression of Cx 32 was observed along the BC (B–D insets), whereas no expression of Cx 32 was observed in the flat cells (F). Scale bar, 50 μm.

hepatocyte couplets[28] and hepatocyte spheroids.[1,47] In the present experiment the morphology of BC networks treated with CB dramatically changed to induce marked dilations of BC. This result showed morphological phenomena similar to those observed when 5.0 μg/ml CB was infused through portal vein and saccular dilatations of BC were induced in the liver.[46] Immunocytochemical staining also revealed that CB treatment caused wide spaces between actin filaments

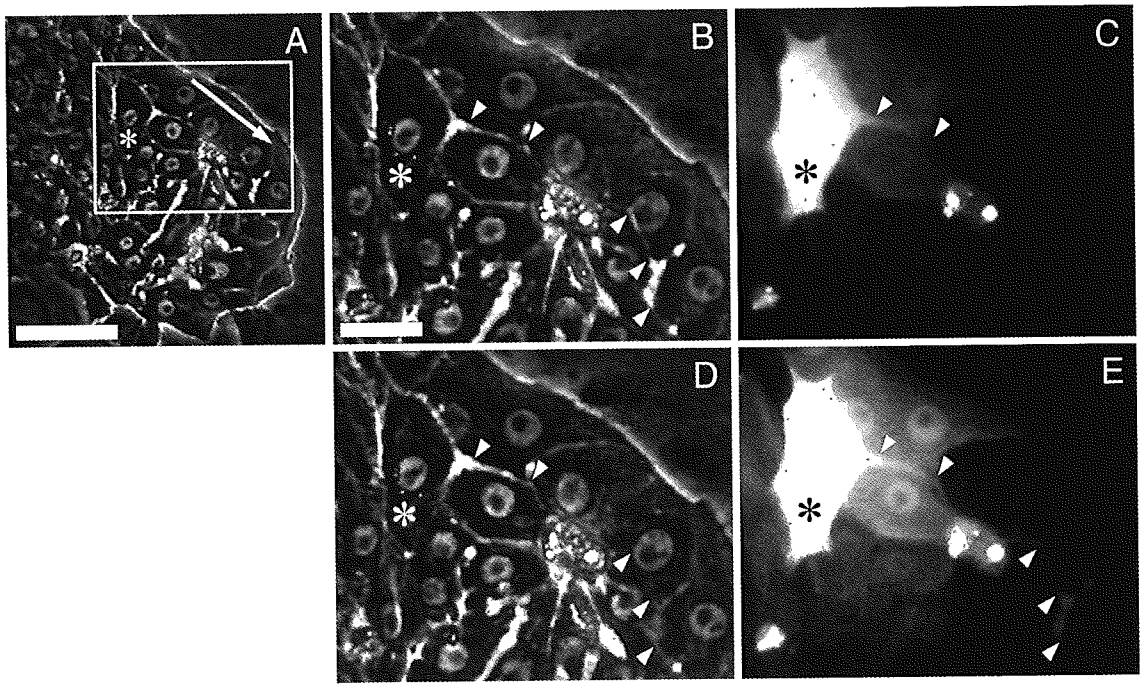

FIGURE 9. Fluorescent images of microinjected dye in the piled-up cells reconstructing BC. CMFDA was microinjected in a cell (asterisk, A) and the fluorescent image was immediately photographed (C). One time-lapse image (2.5 min after C) is shown in (E). Phase-contrast photographs corresponding to the fluorescent images C and E are shown in B and D, respectively. The arrow shows the observed direction of fluorescein transportation. The arrowheads show the fluorescent line secreted from an injected cell. The transported fluorescein within BC is elongated to the tip of the colony (arrowheads, C, E). Scale bars, 50 μm (A) and 20 μm (B).

around BC. The pericanalicular actin filaments were present around dilated BC. These results are consistent with the dilations of BC observed under phase-contrast microscopy.

These results may indicate the involvement of actin filaments in the mechanism of BC contraction. Actin filaments can interact with myosin, which is regulated by Ca^{2+}-calmodulin-dependent phosphorylation. In hepatocytes, myosin is abundant around BC, and the colocalization of actin and myosin was reported in a model of an isolated BC compartment.[41] In addition, ML-9, a myosin light-chain inhibitor, inhibited BC contraction in hepatocyte couplets.[42] Thus, BC contraction may be achieved by coordination of the actin-myosin system, which is regulated by second messengers via gap junctions.

BC Movements and the Flow Within BC

Although the triggers of the BC contractions are still unclear, some possibilities surfaced in the present experiment. (1) The BC contractions could have occurred when the contents of BC were regurgitated into cytoplasm, observed as diacytotic vacuoles. Kawahara *et al.*[9] reported that such regurgitation, called diacytosis,[13] was observed during BC contractions. In this study, similar diacytotic vacuoles were often observed when BC formed in SH colonies contracted. Some small vacuoles were budding off from the BC and this process was simultaneously seen in several parts of BC networks. We previously reported that the tight junctional protein ZO-1 was well expressed along the BC and that accumulated bilirubin did not leak from BC even a few days after the treatment.[35] The results suggested that the reconstructed BC was tightly sealed by the junctions. Therefore, when the pressure in the canalicular lumen was rapidly increased by contractions, biliary content was directed into hepatic cytoplasm and showed diacytosis. (2) The cytokinesis of the cells consisting of BC networks seems to be a trigger for BC contraction. Analysis of the time-lapse movie revealed that BC contractions were sometimes synchronized with the timing of cytokinesis. When the cells that form BC are dividing, the BC may be transiently deformed and the luminal pressure near the region may increase. The increase of the pressure may induce the contraction.

Luminal contents of the BC network need to move because hepatocytes may secrete bile-like substances into motile BC. In this culture the BC networks were closed. Therefore, luminal contents gathered at certain regions and formed cyst-like structures. These often formed at the peripheral regions of the piled-up colonies because BC networks were gradually developed coinciding with the development of the piled-up colonies. The formation of cystic structures may facilitate BC contractions and the canalicular flow. In fact visual analysis of the time-lapse movie showed the flow of luminal contents directed to the cystic structure. Quantified measurement of BC contractions also confirmed this phenomenon [Figs. 5(D–F)]. BC contractions in the root parts of the piled-up colonies caused dilation of BC in the peripheral regions of the colony [Fig. 5(E)], which indicates negative correlation, confirmed by the values of correlation coefficients (p5, Table 2).

BC movements revealed various characteristics. All BC moved, although various speeds of contraction and dilation were observed (Table 1). Analysis of correlation coefficients revealed that BC had both positive and negative correlations. These results indicate that some BC synchronously contract or dilate, and some BC dilate as a result of the contraction of neighboring BC. Although BC is thought to act as a peristaltic pump, both types of movement can transfer their contents. When the cells were treated with CB, dilations of BC were observed particularly in the peripheral regions of the piled-up colonies (Fig. 6). In addition, microinjection studies revealed that the dye secreted from injected cells had a tendency to flow toward the peripheral regions of the piled-up colonies (Fig. 9). These results suggest that secreted bile may be transferred to the peripheral regions by the two types of contractions.

Reconstructing well-assembled hepatic tissues is valuable for tissue engineering of the liver because these tissues can maintain hepatic functions during long-term culture and can be useful for bioartificial livers or tissue-engineered organ transplantation. Although the functions of individual cells have been well analyzed, multicellular functions such as coordination of BC movements have not been investigated. In the present experiment we analyzed BC movements in the organoids and verified coordination of the movements. Therefore, hepatic organoids reconstructed by SHs have potential for the tissue engineering of the liver, and this culture system is a useful model to investigate how the cells are integrated into the tissue.

ACKNOWLEDGMENTS

This work was partially supported by a Grant-in-Aid for Scientific Research in Priority Areas and the 21st Century COE program. We thank Mr. Kim Barrymore for help with the manuscript.

REFERENCES

[1]Abu-Absi, S. F., J. R. Friend, L. K. Hansen, and W. S. Hu. Structural polarity and functional bile canaliculi in rat hepatocyte spheroids. *Exp. Cell. Res.* 274:56–67, 2002.

[2]Brown, S. S., and J. A. Spudich. Mechanism of action of cytochalasin: Evidence that it binds to actin filament ends. *J. Cell Biol.* 88:487–491, 1981.

[3]Clair, C., C. Chalumeau, T. Tordjmann, J. Poggioli, C. Erneux, G. Dupont, and L. Combettes. Investigation of the roles of Ca^{2+} and $InsP_3$ diffusion in the coordination of Ca^{2+} signals between connected hepatocytes. *J. Cell Sci.* 114:1999–2007, 2001.

[4]Cooper, J. A. Effects of cytochalasin and phalloidin on actin. *J. Cell Biol.* 105:1473–1478, 1987.

[5]Fausto, N. Liver regeneration. *J. Hepatol.* 32:19–31, 2000.

[6]Flanagan, M. D., and S. Lin. Cytochalasins block actin filament elongation by binding to high affinity sites associated with F-actin. *J. Biol. Chem.* 255:835–838, 1980.

[7]Hayakawa, T., R. Bruck, O. C. Ng, and J. L. Boyer. DBcAMP stimulates vesicle transport and HRP excretion in isolated perfused rat liver. *Am. J. Physiol.* 259:G727–G735, 1990.

[8]Kamimura, Y., N. Sawada, M. Aoki, and M. Mori. Endothelin-1 induces contraction of bile canaliculi in isolated rat hepatocytes. *Biochem. Biophys. Res. Commun.* 191:817–822, 1993.

[9]Kawahara, H., and S. W. French. Role of cytoskeleton in canalicular contraction in cultured differentiated hepatocytes. *Am. J. Pathol.* 136:521–532, 1990.

[10]Koide, N., K. Sakaguchi, Y. Koide, K. Asano, M. Kawaguchi, H. Matsushima, T. Takenami, T. Shinji, M. Mori, and T. Tsuji. Formation of multicellular spheroids composed of adult rat hepatocytes in dishes with positively charged surfaces and under other nonadherent environments. *Exp. Cell. Res.* 186:227–235, 1990.

[11]Landry, J., D. Bernier, C. Ouellet, R. Goyette, and N. Marceau. Spheroidal aggregate culture of rat liver cells: Histotypic reorganization, biomatrix deposition, and maintenance of functional activities. *J. Cell Biol.* 101:914–923, 1985.

[12]LeCluyse, E. L., K. L. Audus, and J. H. Hochman. Formation of extensive canalicular networks by rat hepatocytes cultured in collagen-sandwich configuration. *Am. J. Physiol.* 266:C1764–C1774, 1994.

[13]Matter, A., L. Orci, and C. Rouiller. A study on the permeability barriers between Disse's space and the bile canaliculus. *J. Ultrastruct. Res.* 11:1–71, 1969.

[14]Michalopoulos, G. K., W. C. Bowen, K. Mule, and D. B. Stolz. Histological organization in hepatocyte organoid cultures. *Am. J. Pathol.* 159:1877–1887, 2001.

[15]Michalopoulos, G. K., W. C. Bowen, V. F. Zajac, D. Beer-Stolz, S. Watkins, V. Kostrubsky, and S. C. Strom. Morphogenetic events in mixed cultures of rat hepatocytes and nonparenchymal cells maintained in biological matrices in the presence of hepatocyte growth factor and epidermal growth factor. *Hepatology* 29:90–100, 1999.

[16]Michalopoulos, G. K., and M. C. DeFrances. Liver regeneration. *Science* 276:60–66, 1997.

[17]Mitaka, T., T. Kojima, T. Mizuguchi, and Y. Mochizuki. Growth and maturation of small hepatocytes isolated from adult rat liver. *Biochem. Biophys. Res. Commun.* 214:310–317, 1995.

[18]Mitaka, T., M. Mikami, G. L. Sattler, H. C. Pitot, and Y. Mochizuki. Small cell colonies appear in the primary culture of adult rat hepatocytes in the presence of nicotinamide and epidermal growth factor. *Hepatology* 16:440–447, 1992.

[19]Mitaka, T., F. Sato, S. Ikeda, S. Sugimoto, N. Higaki, K. Hirata, W. H. Lamers, and Y. Mochizuki. Expression of carbamoylphosphate synthetase I and glutamine synthetase in hepatic organoids reconstructed by rat small hepatocytes and hepatic nonparenchymal cells. *Cell Tissue Res.* 306:467–471, 2001.

[20]Mitaka, T., F. Sato, T. Mizuguchi, T. Yokono, and Y. Mochizuki. Reconstruction of hepatic organoid by rat small hepatocytes and hepatic nonparenchymal cells. *Hepatology* 29:111–125, 1999.

[21]Mitaka, T., G. L. Sattler, H. C. Pitot, and Y. Mochizuki. Characteristics of small cell colonies developing in primary cultures of adult rat hepatocytes. *Virchows. Arch. B. Cell Pathol. Incl. Mol. Pathol.* 62:329–335, 1992.

[22]Miyairi, M., C. Oshio, S. Watanabe, C. R. Smith, I. M. Yousef, and M. J. Phillips. Taurocholate accelerates bile canalicular contractions in isolated rat hepatocytes. *Gastroenterology* 87:788–792, 1984.

[23]Nathanson, M. H., A. D. Burgstahler, and M. B. Fallon. Multistep mechanism of polarized Ca^{2+} wave patterns in hepatocytes. *Am. J. Physiol.* 267:G338–G349, 1994.

[24]Nathanson, M. H., A. D. Burgstahler, A. Mennone, M. B. Fallon, C. B. Gonzalez, and J. C. Saez. Ca^{2+} waves are organized among hepatocytes in the intact organ. *Am. J. Physiol.* 269:G167–G171, 1995.

[25]Nathanson, M. H., L. Rios-Velez, A. D. Burgstahler, and A. Mennone. Communication via gap junctions modulates bile secretion in the isolated perfused rat liver. *Gastroenterology* 116:1176–1183, 1999.

[26]Oshio, C., and M. J. Phillips. Contractility of bile canaliculi: Implications for liver function. *Science* 212:1041–1042, 1981.

[27]Phillips, M. J., C. Oshio, M. Miyairi, H. Katz, and C. R. Smith. A study of bile canalicular contractions in isolated hepatocytes. *Hepatology* 2:763–768, 1982.

[28]Phillips, M. J., C. Oshio, M. Miyairi, and C. R. Smith. Intrahepatic cholestasis as a canalicular motility disorder. Evidence using cytochalasin. *Lab. Invest.* 48:205–211, 1983.

[29]Phillips, M. J., C. Oshio, M. Miyairi, S. Watanabe, and C. R. Smith. What is actin doing in the liver cell? *Hepatology* 3:433–436, 1983.

[30]Roelofsen, H., C. J. Soroka, D. Keppler, and J. L. Boyer. Cyclic AMP stimulates sorting of the canlicular organic anion transporter (Mrp2/cMoat) to the apical domain in hepatocyte couplets. *J. Cell Sci.* 111:1137–1145, 1998.

[31]Saez, J. C., J. A. Connor, D. C. Spray, and M. V. Bennett. Hepatocyte gap junctions are permeable to the second messenger, inositol 1,4,5-trisphosphate, and to calcium ions. *Proc. Natl. Acad. Sci. U.S.A.* 86:2708–2712, 1989.

[32]Seglen, P. O. Preparation of isolated rat liver cells. *Methods Cell Biol.* 13:29–83, 1976.

[33]Serriere, V., B. Berthon, S. Boucherie, E. Jacquemin, G. Guillon, M. Claret, and T. Tordjmann. Vasopressin receptor distribution in the liver controls calcium wave propagation and bile flow. *FASEB. J.* 15:1484–1486, 2001.

[34]Smith, C. R., C. Oshio, M. Miyairi, H. Katz, and M. J. Phillips. Coordination of the contractile activity of bile canaliculi. Evidence from spontaneous contractions *in vitro*. *Lab. Invest.* 53:270–274, 1985.

[35]Sudo, R., S. Ikeda, S. Sugimoto, K. Harada, K. Hirata, K. Tanishita, Y. Mochizuki, and T. Mitaka. Bile canalicular formation in hepatic organoid reconstructed by rat small hepatocytes and nonparenchymal cells. *J. Cell Physiol.* 199:252–261, 2004.

[36]Sugimoto, S., T. Mitaka, S. Ikeda, K. Harada, I. Ikai, Y. Yamaoka, and Y. Mochizuki. Morphological changes induced by extracellular matrix are correlated with maturation of rat small hepatocytes. *J. Cell. Biochem.* 87:16–28, 2002.

[37]Sundback, C. A., and J. P. Vacanti. Alternatives to liver transplantation: From hepatocyte transplantation to tissue-engineered organs. *Gastroenterology* 118:438–442, 2000.

[38]Talamini, M. A., B. Kappus, and A. Hubbard. Repolarization of hepatocytes in culture. *Hepatology* 25:167–172, 1997.

[39]Tordjmann, T., B. Berthon, M. Claret, and L. Combettes. Coordinated intercellular calcium waves induced by noradrenaline in rat hepatocytes: Dual control by gap junction permeability and agonist. *EMBO J.* 16:5398–5407, 1997.

[40]Tordjmann, T., B. Berthon, E. Jacquemin, C. Clair, N. Stelly, G. Guillon, M. Claret, and L. Combettes. Receptor-oriented intercellular calcium waves evoked by vasopressin in rat hepatocytes. *EMBO J.* 17:4695–4703, 1998.

[41]Tsukada, N., and M. J. Phillips. Bile canalicular contraction is coincident with reorganization of pericanalicular filaments and co-localization of actin and myosin-II. *J. Histochem. Cytochem.* 41:353–363, 1993.

[42] Watanabe, S., A. Miyazaki, M. Hirose, M. Takeuchi, H. Ohide, T. Kitamura, T. Ueno, E. Kominami, and N. Sato. Myosin in hepatocytes is essential for bile canalicular contraction. *Liver* 11:185–189, 1991.

[43] Watanabe, S., and M. J. Phillips. Ca^{2+} causes active contraction of bile canaliculi: Direct evidence from microinjection studies. *Proc. Natl. Acad. Sci. U.S.A.* 81:6164–6168, 1984.

[44] Watanabe, S., C. R. Smith, and M. J. Phillips. Coordination of the contractile activity of bile canaliculi. Evidence from calcium microinjection of triplet hepatocytes. *Lab. Invest.* 53:275–279, 1985.

[45] Watanabe, S., M. Tomono, M. Takeuchi, T. Kitamura, M. Hirose, A. Miyazaki, and T. Namihisa. Bile canalicular contraction in the isolated hepatocyte doublet is related to an increase in cytosolic free calcium ion concentration. *Liver* 8:178–183, 1988.

[46] Watanabe, N., N. Tsukada, C. R. Smith, and M. J. Phillips. Motility of bile canaliculi in the living animal: Implications for bile flow. *J. Cell Biol.* 113:1069–1080, 1991.

[47] Yumoto, A. U., S. Watanabe, M. Hirose, T. Kitamura, Y. Yamaguchi, and N. Sato. Structural and functional features of bile canaliculi in adult rat hepatocyte spheroids. *Liver* 16:61–66, 1996.

LIVER TRANSPLANTATION 12:78–87, 2006

ORIGINAL ARTICLE

Liver Repopulation and Long-Term Function of Rat Small Hepatocyte Transplantation as an Alternative Cell Source for Hepatocyte Transplantation

Chihiro Shibata,[1] Toru Mizuguchi,[1] Yamato Kikkawa,[2] Takayuki Nobuoka,[1] Hideki Oshima,[1] Hiroyuki Kawasaki,[1] Masaki Kawamoto,[1] Tadashi Katsuramaki,[1] Toshihiro Mitaka,[2] and Koichi Hirata[1]

[1]Department of Surgery I, Sapporo Medical University Hospital, Sapporo, Hokkaido, Japan; and [2]Department of Pathophysiology, Cancer Research Institute, Sapporo Medical University School of Medicine, Sapporo, Hokkaido, Japan

Hepatocyte transplantation (HT) is an attractive therapeutic modality for liver disease as an alternative for liver organ transplantation. Primary fresh hepatocytes (FHs) are the exclusive cell source that has been used for clinical HT. However, the use of FHs is limited due to a shortage of donor cells. Small hepatocytes (SHs) are hepatic progenitor cells and can be isolated not only from rodents but also from humans. SHs can proliferate in vitro and express liver functions, although conventional hepatocytes lose them within a short period after culture. SH functions in vivo have never been studied. We therefore investigated HT using SHs to evaluate cell engraftment and function compared to HT using FHs. The donor cell number in the SH group was smaller than that in the FH group at HT. The cell engraftment in the SH group was smaller in the liver and larger in the spleen than in the FH group. The cell engraftment in the liver increased after HT; however, that in the spleen decreased after HT in both groups. HT using SHs supported the serum albumin level in the NAR experiment as well as that using FH, and albumin mRNA was detectable in the recipients' tissues at 12 weeks after HT. In conclusion, HT using SHs showed hepatic repopulation similar to that using FHs. This suggests that both SHs and FHs can repopulate the liver as if they were hepatic stem cells. In addition, HT using SHs supported liver functions such as albumin correction at the same level as that using FHs. These observations strongly support the idea that SHs could be an alternative to primary FHs as a novel cell source for future HT. *Liver Transpl 12:78–87, 2006.* © 2005 AASLD.

Received February 9, 2005; accepted July 14, 2005.

See Editorial on Page 16

Liver transplantation (LT) has become a golden treatment for liver diseases, including inherited metabolic errors, acute liver failure, and chronic liver failure.[1,2] However, the shortage of donor organs is an obstacle for applying LT to every patient. Therefore, hepatocyte transplantation (HT) has been considered as an alternative for LT and has long been investigated.[3,4]

Primary fresh hepatocytes (FHs) are the main cell source not only for experimental investigations but for clinical HT.[5] Other cellular sources such as xenogenic hepatoyctes, fetal hepatocytes, hepatic progenitor cells, and immortalized hepatocytes have been tested in experimental investigations.[3] All these cells

Abbreviations: HT, hepatocyte transplantation; FH, fresh hepatocyte; SH, small hepatocyte; LT, liver transplantation; DPPIV, dipeptidyl peptidase IV; SD, Sprague-Dawley; NAR, Nagase analbuminemic rats; DMEM, Dulbecco's modified Eagle's medium; FBS, fetal bovine serum; Asc2P, ascorbic acid 2-phosphate; EGF, epidermal growth factor; DMSO, dimethyl sulfoxide; BrdU, 5-bromo-2′-deoxyuridine; PCR, polymerase chain reaction; SD, standard deviation; SDS, sodium dodecyl sulfate.

Supported by Grants-in-Aid from the Ministry of Education, Culture, Sports, Science and Technology, Japan 15790696 for T. Mizuguchi, and 13557107 for K. Hirata. Part of this study was also supported by funds from the Sumitomo Trust for T. Mizuguchi.

Address reprint requests to Toru Mizuguchi, MD, PhD, Department of Surgery I, Sapporo Medical University School of Medicine, S-1, W-16, Chuo-Ku, Sapporo, Hokkaido 060-8543, Japan. Telephone: 81-11-611-2111 (ext. 3281); FAX: 81-11-613-1678; E-mail: tmizu@sapmed.ac.jp

DOI 10.1002/lt.20558
Published online in Wiley InterScience (www.interscience.wiley.com).